Optical structure factor measurements of soot particles in a premixed flame

S. Gangopadhyay, I. Elminyawi, and C. M. Sorensen

We have measured the scattered-light intensity as a function of the scattering angle for light scattered from soot particles in a premixed methane/oxygen flame. This yields the optical structure factor for the soot particles. We find that the structure factor shows the soot particles to have a morphology consistent with a fractal interpretation with a fractal dimension in the $1.6 \lesssim D \lesssim 1.8$ range and a radius of gyration that increases with the height above the burner. The structure factor may also show the effect of the finite monomer size of the soot clusters.

Key words: Particle sizing, soot, fractal morphology.

Introduction

Considerable effort has been spent in the past to develop *in situ* optical techniques to determine the characteristics of soot particles in a flame. The past two decades have seen the development of two major techniques for optical particle sizing, which may be classified as static, scattering/extinction methods[1,2] and dynamic light-scattering methods.[3-8] The static methods rely on Mie-scattering theory, usually in the small-particle Rayleigh limit, to interpret scattered intensity and optical turbidity (extinction) measurements made on the flame. The method, as refined by D'Allesio and co-workers,[1,2] relies on the fact that carbonaceous soot has a complex index of refraction. Because of this, scattering and turbidity measurements have different dependencies on size and number density, thus allowing these two quantities to be extracted. This method has seen extensive application to fundamental studies of soot nucleation and growth. More recently, dynamic light scattering has been applied to soot particle sizing.[3-8] This method measures the scattered-light intensity autocorrelation function from which the particle diffusion coefficient can be obtained. Knowledge of gas temperature and viscosity then allows one to determine a mean hydrodynamic size of the particles. This method does not rely on knowledge of the particles' refractive index, is pointwise, and can be used to gain information on the size distribution, but it does not yield a number density.

A major problem with both of these techniques is that they do not contend with the seemingly random, chainlike nature of the soot particle aggregates as seen in electron microscope studies. The scattering/extinction methods measure a volume equivalent sphere for the aggregate, whereas the dynamic methods measure an effective hydrodynamic radius. Indeed, during the early development of either method, our understanding of such ramified clusters did not allow for a quantitative description of their morphology. This lack of understanding has changed dramatically in the last decade with the discovery by Forrest and Witten[9] that cluster aggregates have a fractal morphology with a characteristic fractal dimension. Since then, numerous studies have illustrated the fractal morphology of aggregates generated either by the computer or in the real world.[10,11]

A fractal may be defined as an object with scale-invariant symmetry; i.e., it looks the same on a variety of length scales.[12] For clusters a consequence of this scale invariance is that the number of monomer units N in a cluster scales with the cluster radius of gyration R_g as

$$N \sim R_g^D, \tag{1}$$

where D is a noninteger fractal dimension. Another consequence of the scale invariance is a power-law density autocorrelation function. The Fourier transform of this quantity is the structure factor $S(q)$ for

The authors are with the Department of Physics, Cardwell Hall, Kansas State University, Manhattan, Kansas 66506-2601.

Received 5 July 1990.
0003-6935/91/334859-06$05.00/0.

scattered radiation, and it too is a power law of the form[13,14]

$$S(q) \sim \mathbf{q}^{-D}, \tag{2}$$

where $\mathbf{q} = (4\pi/\lambda) \sin \theta/2$ is the scattering wave vector. This holds for $\mathbf{q}R_g > 1$, but $S(q)$ is constant for $\mathbf{q}R_g < 1$, and this crossover can be used to determine R_g. Since length scales in typical colloidal or aerocolloidal clusters range from ~10 nm for the monomer size to a few hundred nanometers for the cluster size, an appropriate radiation to make structure factor measurements on fractal aggregates is light. Thus a number of optical structure factor measurements have been used to determine the fractal morphology and D for colloidal particles in a liquid suspension.[10,11,15]

Given this background, the application of optical structure factor measurements to soot particles is a reasonable goal. Two such studies have appeared, one on silica particles in a flame[16] and one on flame-generated carbonaceous particles in an aerosol.[17] Both showed the aggregates to be fractal. Recently, theoretical studies have refined our knowledge of the optical structure factor for such particles.[13,14,18] In particular Mountain and Mulholland[14] have used computer-generated particles to simulate the scattered-light intensity from an ensemble of such particles.

Our purpose is to describe *in situ* optical structure factor measurements for soot particles in a premixed flame and demonstrate their usefulness. Our method is born by analogy to earlier work on colloids and the results of Mountain and Mulholland. From these measurements we determine R_g and D. We find that precise values for R_g can be obtained. We also find that reasonable values of D can be obtained, but larger experimental values of the scattering wave vector would narrow the uncertainty.

Experimental Method

Our flame was supported on a cooled porous frit burner obtained from McKenna Products. The premixed gases passed through a frit 6 cm in diameter. This frit was surrounded by an annular sheath region 0.5 cm wide through which nitrogen was passed. A steel stagnation plate 15 cm in diameter was placed 30 mm above the burner surface to stabilize the flame. The burner was mounted on a translation stage for adjustment.

The gases used were methane and oxygen premixed before the burner. Their flows were controlled by critical orifices that we calibrated with a dry-test flowmeter. The cold gas velocity, uniform across the frit, of the mixture was 6 cm/s. The nitrogen sheath flow was also a critical orifice controlled to a velocity of 5 cm/s. This arrangement yielded a quasi-one-dimensional (1-D) flame with the only major variable being the height above the burner h. The fuel-to-oxidizer ratio of these flames is described by the ratio of carbon atoms to oxygen atoms (C/O) in the gas mixture. We used two ratios: C/O = 0.69 and 0.75. The C/O ratio for complete combustion to H_2O and CO_2 is 0.25.

The flatness, i.e., the uniformity across a given diameter, is an important consideration in structure factor measurements. We measured the scattered light intensity at a scattering angle of 90° across a number of chords of the cylindrical flame. This was done by moving the burner parallel to the incident beam, which was along a diameter of the flame in what we designate the x direction. The detector looked in at 90° along various chords of the cylindrical flame as x varied. An example of these measurements is given in Fig. 1. These data are similar to the quantitative calculations we have performed that model this measurement from an assumed flat flame of various densities. These model calculations indicate that the uniform decrease in scattered intensity as a function of distance in the center 4 cm is due to the turbidity of the flame and the increasing total path length of incident plus scattered light as x increases. The peaks at the edges were also seen in the model calculations and are due to the total path length's sharp decrease at the edges. Minor edge effects are probably also important here. Hence we found that our flames were flat. This is important because as the scattering angle θ is decreased, the length of the scattering volume increases as $1/\sin\theta$. Any bumps or irregularities would then be convoluted in as θ varied, and hence extra θ dependencies are added beyond those found in the structure factor. A flat flame insures that the only θ dependencies are due to the structure of the particles.

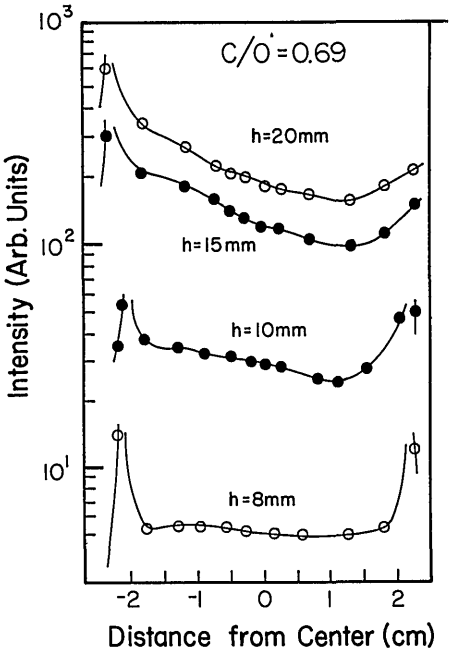

Fig. 1. Intensity scattered at $\theta = 90°$ as a function of the distance from the center of the burner to the scattering volume x. The incident beam is along the x axis. Intensities at the height above burner h = 8 and 10 mm have been multiplied by 2 and 3, respectively.

Whereas the flame may be flat, i.e., uniform in that the same soot is found everywhere along the beam at a given height, the turbidity does change the scattered intensity along the beam. Thus as θ decreases the scattered signal becomes an average over a wider range of x, hence a wider range of scattered intensities. If we keep the scattering volume small, the region of averaging, i.e., the length of the scattering volume, will see a linear variation of the scattering intensity. Thus the average will not be a function of θ, which is what we desire.

Our light-scattering apparatus used an argon-ion laser operating at $\lambda = 488$ nm as a source. The vertically polarized light was focused by a 50-cm focal length lens into the flame. The burner was mounted on an *xyz*-translation stage over the pivot of our goniometer. This was an optical rail 1 m long. This rail rotated about the pivot on a flat optical table. Mounted on the rail was a 10-cm focal length collection lens that imaged the incident beam onto an iris diaphragm with unity magnification. This gave us a scattering volume 1 mm long at 90°. Light passing through this iris diaphragm then passed through a 488-nm notched filter to eliminate the blackbody light from the hot soot. Detection was made with an ITT FW130 photomultiplier tube. Its analog output was converted to a digital signal, which was read by a personal computer. Values of the scattered light were sampled once per second with 1-s integration times. The variation between samples was usually $<1\%$.

It was necessary to take care for accurate alignment of the goniometer. First, adjustment was made so that the incident beam passed directly over the center of the burner and that this center was directly over the pivot. If this latter condition was not satisfied, the position of the detected scattering volume would change with θ. This then caused an artificial change in the scattered intensity as a function of θ, which is unacceptable. The zero angle was determined by allowing the incident laser beam to pass through the collection apparatus (a reflex mirror just before the cathode protected the photomultiplier tube). Then angles were measured and marked relative to this zero. Eleven scattering angles, which ranged between 10 and 115° ($0.087 \leq \sin\theta/2 \leq 0.84$), were used in these experiments.

After a flame of a given C/O ratio was ignited, it was allowed to stabilize for ~5 min. The stagnation plate was cleaned of built-up soot before a given run. Then the lowest height, $h = 8$ mm, was selected, and the intensity as a function of θ was measured sequentially through the 11 angles. This took ~1 min and was repeated 3 times. The scattered intensity fell at most ~2% between each angle sweep owing most likely to the buildup of soot on the stagnation plate. The three sets of data were shifted by these small percentages to provide maximum overlap between them. The values of the intensity were then averaged and corrected for the change in scattering volume as θ varied by multiplying by $\sin\theta$. The apparent random error of the three shifted intensities at any given angle was usually ~1%. Higher heights were then measured after cleaning the stagnation plate. Repeating lower heights at later times showed good reproducibility to 3%.

The results for the scattered intensity $I(q)$ as a function of the scattering-wave vector are given in Figs. 2 and 3 for the two C/O ratios studied. One can see that the data are quite regular and uniform. Also the shapes are as expected for fractal aggregates when $\mathbf{q}R_g \sim 1$, a flat q-independent region at low q curving over at higher q to graphs that appear to be approaching a constant slope to indicate the power law q^{-D} on these log–log plots.

Analysis

The structure factor for light scattered from fractal aggregates has been calculated,[13,18] and these forms can be well approximated by[19]

$$S(q) = S(o)\,(1 + 2q^2R_g^2/3D)^{-D/2}. \tag{3}$$

In Eq. (3) $\mathbf{q}$ is the scattering-wave vector

$$\mathbf{q} = 4\pi\lambda^{-1}\sin\theta/2, \tag{4}$$

where θ is the scattering angle. The functional form of $S(q)$ depends on both the power-law decay of the density–density correlation function and the way this correlation function cuts off at the edge of the aggregate. While the correlation function is the same for all fractal aggregates, the cutoff function is model dependent. Equation (3), which has a modified Fisher–Burford form, is a good approximation to the exact $S(q)$ obtained when an exponential cutoff is used. The computer-generated clusters of Mountain and Mulholland had a faster cutoff than exponential, and their $S(q)$ differed slightly from Eq. (3). Fortunately, its value is unimportant in the small qR_g expansion used to determined R_g.

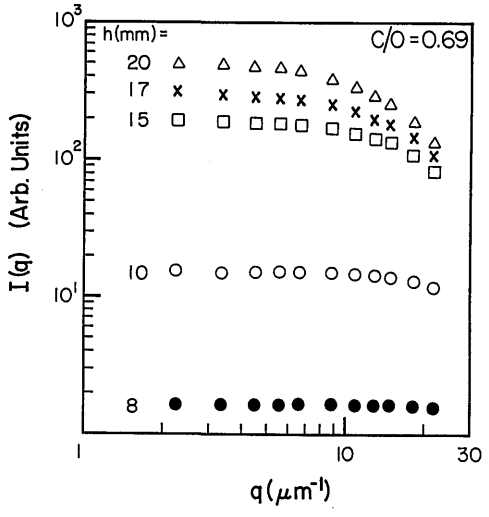

Fig. 2. Scattered light intensity $I(\mathbf{q})$ as a function of the scattering wave vector $\mathbf{q}$ for five different heights above burner h for the C/O = 0.69 flame.

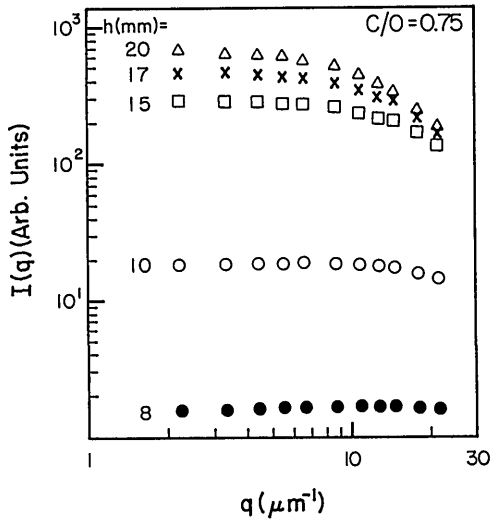

Fig. 3. Scattered light intensity $I(\mathbf{q})$ as a function of the scattering wave vector $\mathbf{q}$ for five different heights above burner h for the C/O = 0.75 flame.

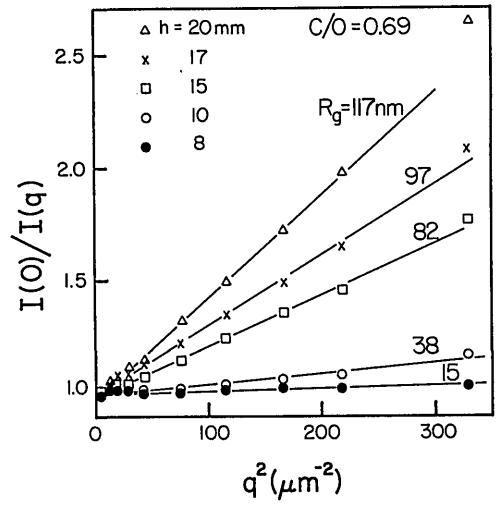

Fig. 4. Graph of the inverse normalized scattering intensity $I(0)/I(\mathbf{q})$ versus wave vector squared $\mathbf{q}^2$ for the C/O = 0.69 flame. Linearity is in accord with Eq. (6), and the slopes yield the R_g values as labeled in the diagram.

The expansion of Eq. (3) for $qR_g \ll 1$, or any $S(q)$ for any cluster morphology fractal or otherwise, yields

$$S(q) \simeq S(0)\,(1 - 1/3\,q^2R_g^2). \tag{5}$$

If we now consider a distribution of particle sizes $n(N)$ in the scattering volume, the total scattered-light intensity $I(q)$ will be

$$I(q) = I(0)\,(1 - 1/3\,q^2\langle R_g^2\rangle), \tag{6}$$

where the brackets imply an intensity weighted average, $\langle R_g^2\rangle \sim \int R_g^2N^2n(N)\mathrm{d}N$. Since we measured $I(q)$ versus q, we made a graph of $I(0)/I(q)$ versus q^2 for each flame. The intensity at our smallest scattering angle, $\theta = 10°$, was used for $I(0)$. Such graphs should be linear with slopes of $\langle R_g^2\rangle/3$.

Figure 4 shows this plot for the C/O = 0.69 flame. The plots are quite linear up to $I(0)/I(q) \sim 2$. Calculation of this ratio with the unapproximated function Eq. (3) with values of D in the $1.5 \le D \le 2.5$ range and then by graphing in the same manner indicated that reasonable linearity would hold until this ratio was ~ 2. Thus we feel secure in using the slopes below $I(0)/I(q) = 2$ to determine R_g. The value of R_g we obtain is a root-mean-square value, $R_g = (\langle R_g^2\rangle)^{1/2}$. We note for $h = 8$ mm that the data barely define a slope within experimental error; hence the error in R_g for this h is relatively large. The values of R_g for both flames as a function of h are plotted in Fig. 5.

Use of the expansion in Eq. (6) eliminates the need to know the fractal dimension to determine R_g. After R_g is measured D can be obtained by using the measured R_g and least-squares fitting the data to Eq. (3). The value of D determined from Eq. (3) is unaffected by the polydispersity as long as the polydispersity is not power law with size. This condition is satisfied for Brownian coagulation, which gives rise to soot aggregates. Our procedure was to combine all the data at all heights for a given C/O in their normalized, $I(q)/I(0)$, form. Equation (3) was then calculated by using the measured R_g values and the experimental q terms and compared to the data. The χ^2 deviation was then determined as a function of D, the minimum yielding the best fit D.

Fits to all the data yielded values of $D = 1.8 \pm 0.2$ for both flames. The experimental error in R_g did not significantly contribute to the error in D. Deviations of 10–20% between data and the fit at the two largest q values for all h were observed. If these last two points were somewhat arbitrarily removed from each run, a fractal dimension, $D = 1.6 \pm 0.15$, was found for each flame. A graphic representation of these fits is given in Fig. 6 where by plotting $I(q)/I(0)$ versus $1 + 2R_g^2q^2/3D$ all the data should collapse to a single

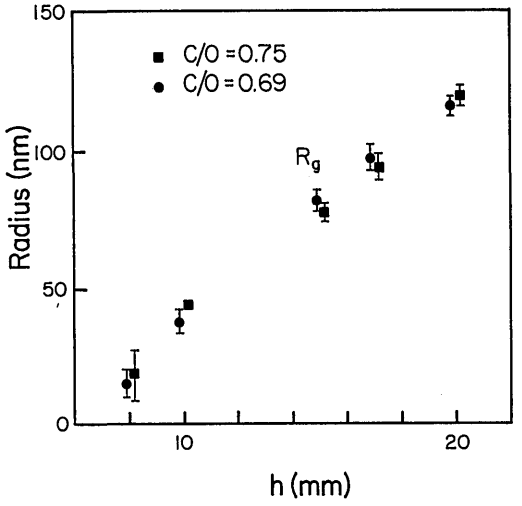

Fig. 5. Soot particle radius of gyration R_g as a function of height above burner h for both flames.

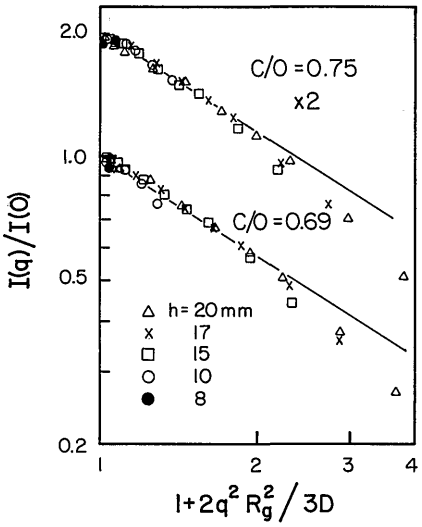

Fig. 6. Graph of the normalized scattering intensity plotted so that the slope is equal to $-D/2$, $D = 1.6$.

curve. The slope on this log–log graph should be $-D/2$ if Eq. (3) is obeyed. The correlation of the data is quite good except for the largest two values of q for each h.

It is possible that this deviation from Eq. (3) is due to the finite monomer size, the radius a. We first note that the deviation is always largest for the largest q for nearly all h. Since the monomer size is not expected to be a strong function of h, this deviation observed at nearly all h fits the monomer suggestion. We may envision the complete structure factor as a product of a fractal part, Eq. (3), and a monomer part.

$$S(q)_{\text{tot}} = S(q)F(aq), \tag{7}$$

where $F(aq)$ is the monomer form factor. The form factor for the spherical monomers is well described by the Rayleigh–Debye theory.[20] Deviation of the normalized Rayleigh–Debye form factor from unity of 10–20% at our two largest q values can be obtained with $a = 30$ nm. This pulls the complete product $S(q)_{\text{tot}}$ down by 10–20% as well, which qualitatively fits our data. The size $a = 30$ nm is slightly larger than the values usually measured in electron microscope studies.[21,22] It would be interesting to probe to larger values of q in the future.

Other than this possible monomer effect correlation of the data to the fractal structure factor is quite good as demonstrated by Fig. 6. We believe that the best values of D are obtained when the apparently deviant large q values are eliminated from the fit, i.e., $D = 1.6 \pm 0.15$. We support this because the reduced χ^2 of these fits is ~30% lower than when all the data are fit, and Eq. (7) can improve the fit by using reasonable values of a. We cannot, however, eliminate the $D = 1.8$ and no-monomer-correction case. We must be realistic and acknowledge that larger values of R_g/a are necessary to obtain a more accurate D or decide on the effects of the finite monomer size. Indeed one can question whether the fractal concept even applies for small R_g/a when $N < 10$.

Our values of D may be compared with both simulation values, which range as $D = 1.7$–1.9,[14,23] and an experiment that uses electron micrograph analysis of captured soot particles, which gave $D = 1.8 \pm 0.1$.[22,24] On the other hand, Hurd and Flower[16] obtained $D = 1.5 \pm 0.15$ in silica flames. Furthermore, in earlier work from this laboratory[17] on soot particles extracted from the same premixed, methane/oxygen flames, analyzed by both electron microscope and structure factor measurements, we found values in the 1.6–1.7 range. Our quoted uncertainty here is due in part to our inability, given our blue light λ, to probe deeply into the $qR_g \gg 1$ regime and the smallness of the R_g/a ratio.

Conclusion

We have presented optical structure factor measurements of soot particles in a premixed flame. The precise radii of gyration R_g of the ramified clusters were obtained from these measurements. The structure factor could be fit well to a fractal form with a fractal dimension in the $1.6 \lesssim D \lesssim 1.8$ range. Some deviation was observed to this fit at large wave vector $\mathbf{q}$, which we have tentatively ascribed to the finite monomer size a. Future work at larger wave vectors should lead to a more accurate value of this monomer size. We believe that optical structure factor measurements provide a valuable new probe for soot particle measurements in a flame without knowledge of the soot index of refraction. It provides new parameters, R_g, D, and a, for quantification of the soot and the study of its origins.

This work was supported by National Science Foundation grant CBT870922.

References

1. A. D'Alessio, A. DiLorenzo, A. F. Sarafim, F. Berretta, S. Masi, and C. Venitozzi, "Soot formation in methane-oxygen flames," in *Fifteenth Symposium (International) on Combustion* (Combustion Institute, Pittsburgh, Pa., 1975), p. 1427.
2. A. D'Alessio, "Laser light scattering and fluorescence diagnostics of rich flames," in *Particulate Carbon*, D. C. Siegla and G. W. Smith, eds. (Plenum, New York, 1981), p. 207.
3. W. Hinds and P. C. Reist, "Aerosol measurement by laser Doppler spectroscopy," Aerosol Sci. **3,** 501–527 (1982).
4. G. B. King, C. M. Sorensen, T. W. Lester, and J. F. Merklin, "Photon correlation spectroscopy used as a particle size diagnostic in sooting flames," Appl. Opt. **21,** 976–978 (1982).
5. S. M. Scrivner, T. W. Taylor, C. M. Sorensen, and J. F. Merklin, "Soot particle size distribution measurements in a premixed flame using photon correlation spectroscopy," Appl. Opt. **25,** 291–297 (1986).
6. W. L. Flower, "Optical measurements of soot formation in flames," Combust. Sci. Technol. **33,** 17–33 (1983).
7. M. E. Weill, P. Flament, and G. Gouesbet, "Diameters and number densities of soot particles in premixed flat flames, propane/oxygen," Appl. Opt. **22,** 2407–2409 (1983).
8. M. E. Weill, N. Lhuissier, and G. Gouesbet, "Mean diameters and number densities of soot particles in premixed flat flames CH_4–O_2 by diffusion broadening spectroscopy," Appl. Opt. **25,** 1676–1683 (1986).
9. S. R. Forrest and T. A. Witten, "Long-range correlations in smoke-particle aggregates," J. Phys. A **12,** L109–L117 (1979).

10. F. Family and D. P. Landau, eds., *Kinetics of Aggregation and Gelation* (North-Holland, Amsterdam, 1984).
11. H. E. Stanley and N. Ostrowsky, eds., *On Growth and Form* (Nijhoff, Boston, 1986).
12. B. Mandelbrot, *The Fractal Geometry of Nature* (Freeman, San Francisco, 1983).
13. T. Freltoft, J. K. Kjems, and S. K. Sinha, "Power-law correlations and finite-size effects in silica particle aggregates studied by small-angle neutron scattering," Phys. Rev. B **33,** 269–275 (1986).
14. R. D. Mountain and G. W. Mulholland, "Light scattering from simulated smoke agglomerates," Langmuir **4,** 1321–1326 (1988).
15. D. W. Schaefer, J. E. Martin, P. Wiltzius, and D. S. Cannell, "Fractal geometry of colloidal aggregates," Phys. Rev. Lett. **52,** 2371–2374 (1984).
16. A. J. Hurd and W. L. Flower, "In situ growth and structure of fractal silica aggregates in a flame," J. Colloid Interface Sci. **122,** 178–192 (1988).
17. H. X. Zhang, C. M. Sorensen, E. R. Ramer, B. J. Olivier, and J. F. Merklin, "In-situ optical structure factor measurements of an aggregating soot aerosol," Langmuir **4,** 867–871 (1988).
18. M. V. Berry and I. C. Percival, "Optics of fractal clusters such as smoke," Opt. Acta **33,** 577–591 (1986).
19. G. Dietler, C. Aubert, D. S. Cannell, and P. Wiltzius, "Gelatin of colloidal silica," Phys. Rev. Lett. **57,** 3117–3120 (1986).
20. M. Kerker, *The Scattering of Light and Other Electromagnetic Radiation* (Academic, New York, 1969).
21. J. Lahaye and G. Prado, "Morphology and internal structure of carbon blacks and soot," in *Particulate Carbon,* D. C. Siegla, and G. W. Smith, eds. (Plenum, New York, 1981), p. 33.
22. R. J. Samson, G. W. Mulholland, and J. W. Gentry, "Structural analysis of soot agglomerates," Langmuir **3,** 272–281 (1987).
23. R. D. Mountain, G. W. Mulholland, and H. J. Baum, "Simulation of aerosol agglomeration in the free molecular and continuum regimes," J. Colloid Interface Sci. **114,** 67–81 (1986).
24. R. A. Dobbins and C. M. Megaridis, "Morphology of flame-generated soot as determined by thermophoretic sampling," Langmuir **3,** 254–259 (1987).